CONF

BNL-29792

CONF-810419--1

PHOTOTHERMAL SPECTROSCOPY OF AEROSOLS

Anthony J. Campillo and Horn Bond Lin

MASTER

Brookhaven National Laboratory
Department of Energy and Environment
Upton, New York 11973

April 1981

Submitted for

Laser Spectroscopy for Sensitive Detection
Proceedings of the Society of Photo-optical Instrumentation Engineers
Vol. 286, 1981.

Under Contract No. DE-AC02-76CH00016 with the
U.S. Department of Energy

286-05

PHOTOTHERMAL SPECTROSCOPY OF AEROSOLS

Anthony J. Campillo and Horn-Bond Lin

Environmental Chemistry Division, Building 426
Brookhaven National Laboratory, Upton, New York 11973

Abstract

In situ aerosol absorption spectroscopy was performed using two novel photothermal detection schemes. The first, based on a photorefractive effect and coherent detection, called 'phase fluctuation optical heterodyne'(PFLOH) spectroscopy, could, depending on the geometry employed, yield particle specific or particle and gas absorption data. Single particles of graphite as small as 1 μm were detected in the particle specific mode. In another geometrical configuration, the total absorption (both gas and particle) of submicron sized aerosols of ammonium sulfate particles in equilibrium with gaseous ammonia and water vapor were measured at varying CO_2 laser frequencies. The specific absorption coefficient for the sulfate ion was measured to be 0.5 m^2/g at 1087 cm^{-1}. The absorption coefficient sensitivity of this scheme was less than or equal to 10^{-8} cm^{-1}. The second scheme is a hybrid visible Mie scattering scheme incorporating photothermal modulation. Particle specific data on ammonium sulfate droplets were obtained. For chemically identical species, the relative absorption spectrum versus laser frequency can be obtained for polydisperse aerosol distributions directly from the data without the need for complex inverse scattering calculations.

Introduction

There has been increasing interest in the absorption properties of airborne particles both as a method of identifying component species (e.g. analytical spectroscopy) and in determining heating effects. An example of the latter is the role of aerosols in heating or cooling of the atmosphere. This is determined largely by scattering and absorption of solar radiation by the particles. This in turn may effect global or local climate. Other examples include several recent proposals for efficient solar collectors based on aerosol absorption. In this paper, we primarily discuss photothermal techniques for measuring atmospheric particles as an aid in species component identification. However, the techniques described herein may in many cases be employed in other particle applications.

An aerosol is defined as a relatively stable suspension of liquid or solid particles in a gas. Nearly all the aerosol mass resulting from chemical reactions in the atmosphere tend to accumulate in airborne particles ranging in diameter from 0.1 to 2 μm.[1] Coincidently , it is within this range of sizes that visible light scattering per unit aerosol mass is at a maximum. Most of the aerosol mass of anthropogenic origin is hygroscopic with a significant fraction consisting of water-soluble salts of nitrate and sulfate. Precise chemical composition information, for example, the relative amounts of sulfate and attached cations, would be of use in understanding various aspects of atmospheric chemistry. Because of the presence of volatile and reactive (e.g. free acids) species in the particles, it would be desirable to employ *in situ* (i.e. in their natural environment) methods of analysis, such as absorption spectroscopy, which do not require the removal of the particles from the air. Several problems have made particle absorption spectroscopy difficult to implement previously. First, direct transmission measurements are complicated by particle light scattering which often obscures the minimal light absorption and second, background gases, such as water vapor, have wing absorptions that dwarf the particulate contribution at ambient levels. As a result, absorption spectroscopy of aerosols in smog chamber studies are usually limited to the gaseous components. Recently, particle absorption measurements overcoming the former problem have been obtained albeit at high concentrations ($\geq$ 1 mg/m^3) on smokes[2] and dusts[3] using photoacoustic spectroscopy, a form of photothermal spectroscopy. However, in these works also, the background gases set a lower limit of sensitivity. In this paper, we describe in detail two promising photothermal schemes that have significant advantages when employed for particle absorption spectroscopy: "Phase Fluctuation Optical Heterodyne" (PFLOH)[4] spectroscopy and photothermally modulated visible Mie scattering. Both can, depending on the geometry and aerosol system chosen for study, yield signals that are particle specific; i.e. independent of background gas absorption.

PFLOH Detection

Recently, a promising photothermal technique for trace gas detection, called "phase fluctuation optical heterodyne" (PFLOH) detection has been demonstrated in pulsed[4] and cw form[5-8]. The anticipated absorption sensitivity of a realistic narrow bandwidth (cw) version of this device appears to be less than 10^{-11} cm^{-1}, superior to the best previously obtained (in the range 10^{-9} to 10^{-10} cm^{-1}) using photoacoustic spectroscopy[9]. Preliminary experimental devices have achieved sensitivities of less than 10^{-8} cm^{-1} in a 'windowless flowing gas mode'[5] and less than 10^{-10} cm^{-1} in a 'windowless static cell'[8]. The flowing gas configuration developed at our laboratory can be conveniently utilized for aerosol characterization. This paper summarizes our initial investigations, which demonstrate the excellent potential of this approach.

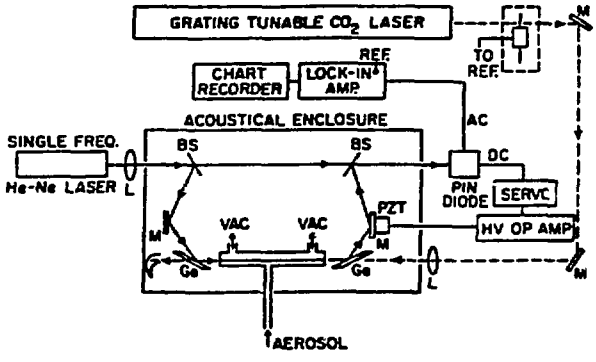

Figure 1. Schematic of experimental PTLOR spectrometer for aerosol studies.

PTLOR detection is calorimetric and yields a signal proportional to the energy absorbed by the sample. For trace gas detection a laser line is chosen which is strongly absorbed by the species of interest. In the absence of absorption saturation and thermal diffusion effects, the energy absorbed is related to the absorption coefficient (and consequently the trace gas concentration), the sample length and the laser intensity. Collisional quenching of the excited species results in heating of the buffer gas, subsequent gas expansion and a change in density and index of refraction. This latter quantity, although small, can be measured by placing the laser-heated sample in a sensitive laser heterodyne interferometer[4-8].

It is instructive to estimate the magnitude of the various quantities involved. If the exciting laser is modulated at frequency, ω_m , it can be shown that the corresponding fourier component of induced index of refraction $\Delta n(t)$ is approximated by

$$\Delta n(t) = \frac{(n-1)\, I_o\, \alpha \sin(\omega_m t)}{2\omega_m C_p T \rho_a} \qquad (1)$$

Here, I_o is the cw intensity of the laser, n is the index of refraction, α the absorption coefficient of the trace species, ρ_a is the density of the sample gas, C_p is the specific heat at constant pressure, and T is the temperature. Equation (1) is derived by assuming that I_o is nonsaturating, that the thermal conduction time is greater than ω_m^{-1} and that the effects of sample cell walls are minimal. For samples in nitrogen, typical values are $\omega_m = 2\pi(27\ Hz)$, T = 293 K, (n-1) = 2.92×10^{-4}, $\rho_a = 1.165 \times 10^{-3}$ g/cm^3, C_p = 1.006 and I = 250 W/cm^2. One ppb ethylene in 1 atm nitrogen excited by the P(14) line of a 10 μm band CO_2 laser (i.e. $P_{10}(14)$, $\alpha = 32.14\ cm^{-1}\ atm^{-1}$)[10], will result in an induced index-change amplitude of $\Delta n = 2 \times 10^{-11}$.

Indices of this magnitude are well within the capability of a coherent laser heterodyne interferometer[4-8]. In this scheme a stable single frequency probe beam, usually from a helium-neon laser source, is utilized in a Mach-Zehnder interferometer[11] containing the sample in one of its arms. This probe beam is split into a reference component and a component to be passed through the sample. The sample probe is consequently phase modulated by the time varying index of refraction and later recombined with the reference beam and heterodyned in a PIN photodiode. The PIN photodiode acts as a nonlinear device (square law detection) and yields a low frequency signal at the difference frequency, corresponding to ω_m. The voltage amplitude, V_H of this component is related to the magnitude of the index of refraction by

$$V_H = V_s \frac{\sin(2\pi L \Delta n(t))}{\lambda} \qquad (2)$$

Here V_s is an experimentally determined electrical calibration constant, L is the sample length and λ the wavelength of the probe laser. In practice the minimum measurable Δn is limited by interferometer vibrations, sample turbulence, window absorption or ultimately the photon noise of the helium neon laser. In a previously described windowless flowing gas cell[3], an absorption coefficient sensitivity of 10^{-8} cm^{-1} was obtained in a 20 cm long sample cell. Since the strongest IR absorption features of many species are typically 10 cm^{-1} atm^{-1}, this implies that concentrations of typically 1 ppb can be detected.

A schematic of our experimental apparatus is shown in Figure 1 above. The excitation laser is a grating tuned flowing $C^{12}O_2^{16}$ gas laser (Holectron model IR250). Multiwatt single line operation can be obtained

on approximately 100 lines in the 9-11 μm range. The beam from this laser is amplitude modulated using a commercial beam chopper (P.A.R. model 25) and enters and leaves the interferometer via two germanium (Ge) Brewster windows. Although transparent at 10.6 μm, the Ge windows form two of the high reflectivity visible mirrors of the interferometer. The interferometer portion of the detector utilizes a relatively inexpensive commercial stable single frequency helium neon laser (Tropel model 100; λ = 633 nm). This particular model laser has been shown to provide an output very close to photon noise limited over a wide frequency range[12]. Both CO_2 beam and helium neon beam overlap in the sample region; the CO_2 beam inducing the index of refraction change and the helium neon beam probing it. The sample is introduced at a constant rate (0.1 to 2 l/min) into a central inlet of an open ended 20 cm long 4 mm I.D. glass capillary tube which served as the sample cell. Vacuum connections were maintained near the tube ends to balance the flow into and out of the cell and to bypass the open ends. A PIN photodiode (EG&G model HAD 1000) is used to process the heterodyned beams and the signal component at the chopping frequency is synchronously detected in a lock-in amplifier (PAR model 128A). The interferometer consists of 6 reflectors, two of which are 50/50 beam splitters at 633 nm. As the interferometer yields an optimum (linear) response midway between destructive and constructive interference, this phase condition is maintained using a servo control system which drives a transducer displacing one of the interferometer mirrors. The PTLOH device was vibrationally and acoustically isolated by means of an air suspension table (NRC model BS-510-8) and an aluminum box enclosure.

The absorption sensitivity of our system was calibrated by flowing a 10 ppb ethylene in nitrogen sample directly through our detection cell(see Figure 2). Based on the observed detection limit (≈ 300 ppt C_2H_4 at S/N = 1), the limiting sensitivity was again determined to be 10^{-8} cm^{-1}, consistent with the above estimate and with a previously published result[3]. The observed signal, 20 μv, was in reasonable agreement with the value of 28 μv calculated using equations (1) and (2) and the values I = 250 W/cm^2 and V_s = 70 mv. The value of V_s was experimentally determined by impressing a ramp voltage upon the interferometer mirror transducer (PZT) and observing the PIN photodiode voltage change due to the resulting optical path length change; the amplitude of the resulting sinusoidal voltage yielded V_s. Some characteristics of our PTLOH detector are summarized in Figures 3 through 5 for gaseous species. A comprehensive theory describing the use of the PTLOH technique in studies of molecular relaxation, thermal conduction and extremely weak absorptions in the gas phase is given by Davis and Patuchowski[6]. A detailed theory of PTLOH detection specific to particle measurements will be presented elsewhere[13] but we outline here some pertinent features.

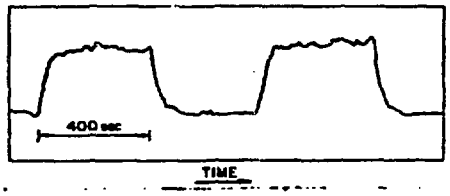

Figure 2. PTLOH signal due to a 25 ml/min flow of 10 ppb C_2H_4 in N_2 under 250 W/cm^2 $P_{10}(14)$ CO_2 laser excitation. The CO_2 laser beam was alternately blocked and unblocked to illustrate the amplitude of the signal and that of the background noise. The fluctuations on the top of the pedestals are due to CO_2 laser power variations and not to system noise.

The heating of a spherical particle exposed to cw laser radiation for times greater than t = 0 has been treated by Chan[14]. The particle heats to an equilibrium temperature, ΔT, above ambient, given by $\Delta T = I Q_{abs} a/4 k_a$ in a characteristic time τ given by $\tau = a^2 \rho_p c_p/3 k_a$. Here I is the laser intensity, Q_{abs} is the normalized absorption cross section[15], a the radius of the particle, k_a is the thermal conductivity of surrounding air, ρ_p is the particle density and c_p the specific heat of the particle. For submicron particles, charateristic heating times are less than a microsecond while a 100 μm particle requires several seconds. Thus, photothermal detection schemes which monitor changes in the surrounding buffer gas appear to be quite suitable for the measurement of small particles since heating times of only milliseconds are required to completely heat even micron sized particles and to conduct sufficient heat to the gas. In the limit, $t \to \infty$, the temperature above ambient of the air, ΔT_a, surrounding a single particle irradiated by a laser is given by the spherically symmetric function $\Delta T_a(r) = \Delta T^*(a/r)$ where r is the radial distance from the center of the particle. For finite t, the function is complicated[14] but can be approximated[13] for our purposes at times, $t \gg \tau$, by $\Delta T_a = \Delta T^*(a/r)$ within the limits $a \leq r \leq \sqrt{\kappa t}$ and $\Delta T_a = 0$ for $r > \sqrt{\kappa t}$; i.e. the heated air zone appears to have a boundary which expands due to thermal diffusion and has a radius of $\sqrt{\kappa t}$. Here κ is the thermal diffusivity of air ($\kappa = 0.186$ cm^2/sec). It can be shown[13] that the phase shift of an optical ray passing through this refracting sphere is given by

$$\Delta\phi(R) = \frac{\tau a^2 Q_{abs} I}{\lambda k_a T} \left[\ln\left(\sqrt{\frac{\kappa t}{R^2}}\right)^{\frac{1}{2}} + \left(\frac{\kappa t}{R^2} - 1\right)^{\frac{1}{2}} \right] \qquad (3)$$

where R is the closest radial approach distance of the ray to the particle and T is the ambient temperature. Using equation (3), it can be seen that a 1 μm particle with $Q_{abs} \approx 1$, exposed to a 100 W/cm^2 laser field for 1 msec produces a $\Delta\phi(R)$ on the order of 10^{-2} radians; actually, the exact phase change observed in the

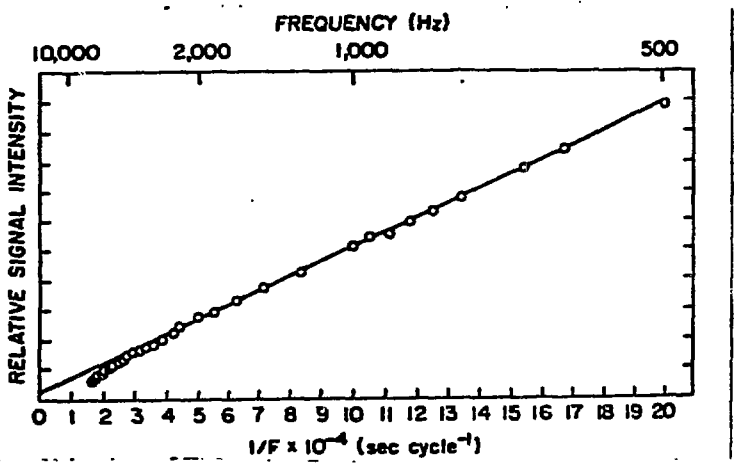

Figure 3. Frequency dependence of PTLOH detection for trace gases

interferometer results from a weighted integration of equation (3) over the spatial profile of the probe He-Ne beam. This phase change is well within the capability of the heterodyne interferometer and implies that single particle sensitivity is achievable for micron sized and possibly smaller particles. Although very small particles ($<< 1\ \mu m$) are not individually distinguishable, collections of them are detectable. Submicron particles heated by a CO_2 laser are in the Rayleigh regime ($a << \lambda$) and the quantity $\pi a^2 Q_{abs}$ is proportional to the mass of the particle. Consequently, the PTLOH signal from an ensemble of small particles will be proportional to their total absorption which is in turn, proportional to their total mass. In general, the formalism describing an ensemble of Rayleigh absorbers observed at t much greater than τ will be very similar to that describing trace gas detection since the energy transfered to the surrounding gas very nearly equals the light energy absorbed. In this case, α in equation (1) can be replaced by the quantity $\alpha + A_s C$, where A_s is the specific absorption coefficient in m^2/g and C is the particulate mass concentration in gram m^{-1}.

PTLOH aerosol detection capabilities in the submicron size range were explored using the apparatus shown in Figure (1). Submicron aerosol particles, generally a polydisperse log normal[15] size distribution with 0.3μm geometric mean diameter and a geometric mean standard deviation of 2, were generated from aqueous ammonium sulfate solution using a TSI model 3076 constant output atomizer[16]. PTLOH spectra for 9 mg/m^3 and 2 mg/m^3 mass concentrations of sulfate are displayed in Figures 6 a and b respectively. Several interesting features should be noted. First, there is a broad absorption feature which increases with decreasing wavenumber due to a particulate absorption band centered at 1110 cm^{-1} and second there are several sharp features due to gaseous absorptions. The gaseous features are more obvious in Figure 6b where the particulate mass concentration has been reduced. The line at 976 cm^{-1} is due to water vapor[17] absorption (approximately 50% humidity) and the line at 1085 cm^{-1} due to NH_3 gas (approximately 500 ppb). Note that the data was obtained in situ on a continuously flowing aerosol and that simultaneous measurements of water vapor and ammonia gas concentration and sulfate mass loading are obtained. This quantitative in situ capability should be useful for direct laboratory aerosol chemistry studies. For example, the buildup of sulfate upon addition of various gases (e.g. SO_2) and catalysts to the aerosol stream will yield needed data concerning the chemistry of sulfates in the atmosphere. An interesting feature of the data shown in figure 6 is the large concentration of NH_3 gas. At no time in our experiments was NH_3 gas added. The observed approximately 500 ppb NH_3 results from chemical equilibrium being established between the $(NH_4)_2SO_4$ water particles and the surrounding air. This point is discussed in detail by Tang[18] and the level of NH_3 observed here is consistent with theory and with our observed relative humidity (50%). We should also mention that the equilibrium partial pressures of nitric acid and ammonia in the atmosphere due to mixed salt aerosol systems is currently a problem of great interest. Using the PTLOH technique described here, measurements of the equilibrium vapor pressure of NH_3 can be extended to various mixed salt systems for which there presently is no available data.

We measured a specific absorption coefficient for sulfate at 1086 cm^{-1} of 0.5 m^2/g and were able to detect sulfate levels as low as 100 $\mu g/m^3$. Measurements of levels below this value were not possible due to background water vapor absorption. Unfortunately, sulfate/ water droplets exist in the atmosphere typically in the range 1-100 $\mu g/m^3$ and consequently ambient sulfate monitoring is not possible with this PTLOH geometry. This geometry should, however, be useful in applications such as diesel exhaust monitoring and in advanced combustion diagnosis where fewer material handling problems are anticipated with this geometry than with, for example, photoacoustic detectors.

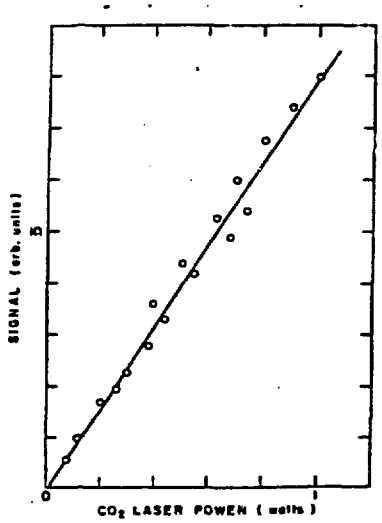

Figure 4. Laser power dependence of PFLOH signal

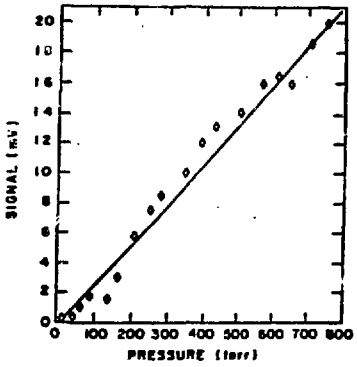

Figure 5. Dependence of PFLOH signal on buffer gas pressure for constant absorption.

Alternative PFLOH geometries can be envisioned to allow the gas signal component to be subtracted from the aerosol signal. We have explored one such geometry which relies on the discrete nature of the particles. This geometry differs from that shown in Figure 1 in three respects. First, the CO_2 laser and the helium neon probe beam are arranged in a 90 degree cross beam geometry in the horizontal plane. Second, the CO_2 laser beam is continuous in time (i.e. not chopped). Third, the aerosol stream is introduced vertically through the intersection of the two beams. The background gas signal being constant in time is effectively subtracted by the servo/PZT system which maintains a phase quadrature relationship between probe and reference beams. As single particles pass through the crossed-beams, phase fluctuations are photothermally induced. The leading edge of the phase perturbation is a ramp function which follows the relation:

$$\frac{\Delta n}{\Delta t} = \frac{4/3\ (n-1)\ a^3\ \rho_p\ A\ I}{C_p\ T\ \rho_a\ w^2 t} \qquad (4)$$

here ρ_p is the density of the particle, w the radius of the helium neon beam and the other parameters as defined previously. Although our results are preliminary, we were able to observe particles of 1 - 10 μm size and the slope of the leading edge was found to agree with equation (4) to within our experimental error (factor of two). We found it convenient to monitor the slope of Δn with respect to time rather than the maximum value of Δn since the residence time of the particles in the interaction region appeared to be a complex function of the size. At this time, we believe that the residence time of the particles is largely determined by photophoresis, the larger particles being radiometrically expelled from the beam at high velocities. At present, sensitivity is limited by mechanical vibrations of the interferometer components and by photophoresis. Vibrations can be minimized by at least two orders of magnitude with a modified Jamin interferometer configuration as demonstrated in reference 8 and it now appears that the absorption of even single submicron particles will be measured in future versions of this apparatus.

Photothermal Modulation of Mie Scattered Light

Visible Mie[15] scattering is a well known phenomenon frequently used to determine physical properties of particles. It is sensitive, in situ and convenient. This scheme normally yields size and index of refraction information. In this section, we describe a photothermal hybrid form of Mie scattering that allows in addition highly sensitive particle absorption spectroscopy to be performed.

A schematic of our experimental apparatus is shown in Figure 7. Submicron aerosol particles were generated as described in the PFLOH section. The resulting aerosol was introduced at constant rate (0 to 2 l/min) into a central inlet of an open ended 20 cm long 4 mm I.D. glass capillary tube which served as the sample cell. Vacuum connections were maintained near the tube ends to balance the flow into and out of the cell and to bypass the open ends. Linearly polarized red (633 nm) light emitted by a Tropel 100 helium neon laser was directed through the sample and elastically scattered off the particles where the horizontally polarized

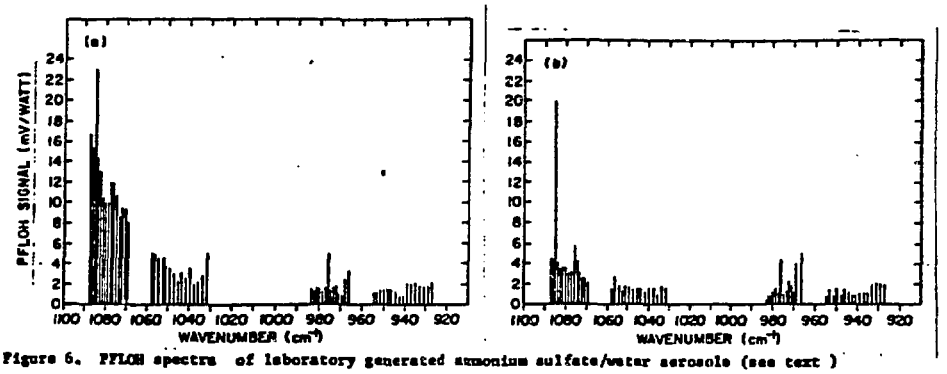

Figure 6. PFLOH spectra of laboratory generated ammonium sulfate/water aerosols (see text)

component was detected at 20 degrees with respect to the forward transmitted beam using an uncooled 1P28 photomultiplier. A grating tunable $^{12}C^{16}O_2$ laser beam, superimposed spatially on the helium neon beam in the sample, was used to modify the visible Mie scattered light. Depending on experimental conditions, modulation amplitudes as high as 40 % (see Figure 8) were observed. At this level, the effect was easily visible to the eye at sub-Hertz chopping rates. Although the modulation amplitude was observed to be linearly proportional to CO_2 laser intensity up to 250 W/cm^2 $R_9(28)$ excitation, the intensity of the CO_2 laser was typically adjusted to keep the modulation amplitude on the order of 1 %. In these circumstances, a lock-in amplifier was employed to synchronously detect the time varying component of the scattered light and the signal displayed using a chart recorder.

There are several mechanisms leading to a photothermal modulation of visible light scattering: (1) photophoresis[19] of the particles out of the illuminating probe beam, (2) macroscopic thermal lensing[20] due to both gas and particle absorption and subsequent distortion of the farfield Mie scattering profile, (3) change in Mie scattering cross-section due to the addition of a localized light refracting heated gas shell surrounding the particle and (4) photothermally induced physical changes(e.g. size, shape) in the particles. For volatile particles, such as mixed salt/water droplets, the dominant mechanism affecting scattered light appears to be size induced changes (evaporation and condensation) as illustrated in Figure 9. For other aerosol species and experimental conditions mechanisms (1) through (3) can be expected to play a contributing role.

Consider the results shown in Figure 8. In this case, ammonium sulfate/water particles were injected into the sample cell and the flow stopped to produce a static aerosol. The 40 % modulation of the scattered light at 0.25 Hz is due to particle heating and subsequent partial evaporation. Note that during the 'off' portion of the CO_2 laser heating cycle, the droplets

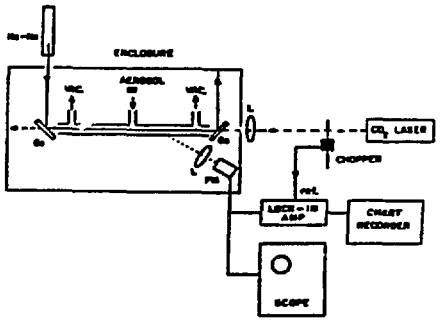

Figure 7. Schematic of photothermally modulated Mie Scattering Apparatus

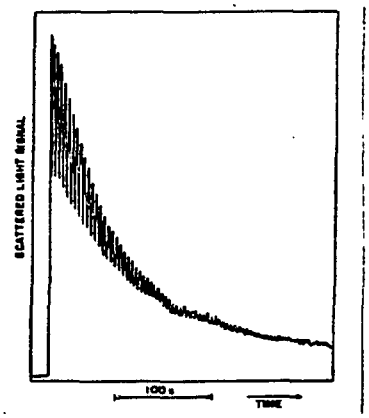

Figure 8. Mie scattered visible light from a static aerosol versus time, when heated by a ½Hz 300 W/cm^2 $R_9(28)$ CO_2 laser beam

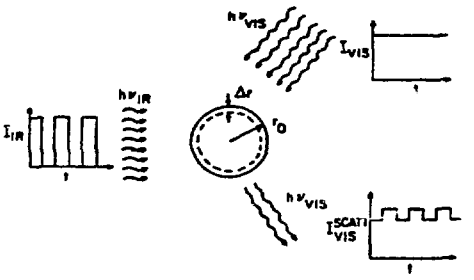

Figure 9. Summary of photothermal modulation of Mie scattering from submicron particles: A chopped infrared source illuminates and heats the volatile particle causing its equilibrium size to fluctuate between the two radii shown. Photons from a cw visible laser are elastically scattered off the particle. The resultant Mie scattered signal contains a time varying component dependent upon the IR absorption cross-section.

recondense to their former size. The longer exponential decay ($\tau \sim 150$ s) of the total light scattering is largely due to photophoresis of the particles out of the field of view of the photomultiplier. Normally, in the absence of CO_2 laser heating, the decay is approximately twice as long and is due to particle diffusion and settling. By maintaining a constant flow of aerosol through the cell, settling, diffusion and photophoresis effects became negligible. The modulation amplitude was independent of chopping frequency for rates up to 300 Hz, suggesting that evaporation and condensation reach equilibrium in times on the order of one millisecond. When 'dry' crystalline ammonium sulfate particles were studied, the scattered light modulation due to size induced changes was eliminated. A somewhat smaller effect was observed in the forward and backward scattered light lobes and whose magnitude, frequency response and angular characteristics appeared consistent with a thermal lens effect due to background water vapor absorption (mechanism 2 above). Mechanism (3) is in general a weak effect at ambient pressure and temperature and could not be observed here.

A theory describing the photothermal modulation of scattered light from volatile particles will be treated elsewhere[21]. We outline here the essential physics. We assume that when exposed to a constant light field, the particle heats within microseconds to an equilibrium temperature that is determined by an energy balance between light absorbed and heat lost through thermal conduction to the surrounding air. Thereafter, the particle modifies its size by evaporation. This approximation was justified by Baker[22], who investigated the effect of radiation on volatile particles by solving the complete hydrodynamic equations. The equilibrium temperature change, ΔT , of a spherical particle above ambient air temperature is given by Chan[14]; $\Delta T = I Q_{abs} a/4 k_a$. Here I_1 is the intensity of the heating laser, Q_{abs} in the IR is the normalized Rayleigh absorption cross-section[15], a is the radius of the particle and k_a the thermal conductivity of the ambient air. For a 0.3 μm diameter droplet illuminated by 250 W/cm^2 of 9.2 μm radiation, ΔT is approximately 0.7 °C. At the elevated temperature, water evaporates from the particle until an equilibrium water: salt ratio is established and the water vapor pressure above the particle surface just equals that of the surrounding air. Tang using thermodynamic arguments[16] has derived an expression relating the equilibrium radius of a solution droplet containing non-volatile multicomponent electrolytes to the temperature T, the relative humidity and to various solution parameters. For particles larger than 0.05 μm , this expression reduces to the well known Raoult's law. If the temperature change is small, the approximation $\Delta a/a = -(3-3X)^{-1}\cdot(\Delta T/T)$ appears justified[21]. Here, X is the mole fraction of water in the droplet and T is the temperature in degree Centigrade. Thus, heating a particle by 1 °C would typically result in a radius change of 8% and a Mie scattering cross-section reduction in the visible of about 24 %. In general, however, size dependent resonances in the Mie scattering process complicates interpretation of the modulation amplitude. The absolute magnitude of the photothermal modulation amplitude of the scattered light will be a strong function of the exact aerosol size distribution encountered, particles in the size range 0.1 to 2 μm tending to contribute more to the scattering process. However, an important point is that an exact expression for the modulation amplitude is separable into multiplicative factors, one of which depends solely on wavelength, the absorption. This factorability results from the IR absorption cross-section per unit mass being independent of the particle size (Rayleigh regime). Consequently, a plot of the modulation amplitude versus laser wavelength for a polydisperse aerosol will yield a true relative absorption spectrum of the particulate matter. Thus, this technique is appropriate for applications requiring determination of the relative composition of particles; for example, the ratio of $(NH_4)^+$ ions: $(SO_4)^=$ ions: H_2O molecules. For a polydisperse aerosol of diverse chemical species of varying sizes, the absorption spectrum will represent a weighted average favoring the more efficient scatterers. Fortunately, this size range, 0.1 to 2 μm , coincides with the chemical product accumulation range in atmospheric aerosols and is of considerable interest.

Figure 10 shows the 920 to 1080 cm^{-1} absorption spectrum of ammonium sulfate particles using this method. This data agrees well with additional data obtained using FTLOH spectroscopy (see Figure 6). The good agree-

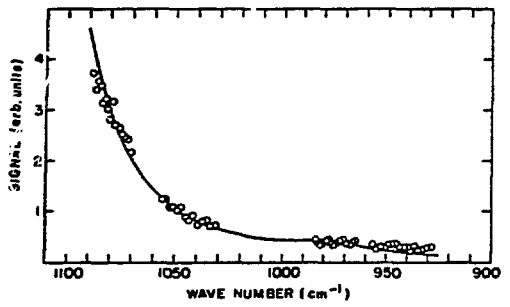

Figure 10. Plot of the time varying component of Mie scattered light versus CO_2 laser frequency for a flowing ammonium sulfate aerosol. The data yields an accurate representation of the particulate infrared absorption spectrum over the frequency range shown.

ment demonstrates that the photothermal scattering technique yields a valid particle relative absorption spectrum. Previous infrared spectra of ammonium sulfate crystals pressed into KBr pellets[23] show a strong $SO_4^{=}$ ion band at 1110 cm^{-1}, as in figure 10, and a weak band at 980 cm^{-1}. Assuming the existence of these bands in the aerosol spectrum, a calculated fit to the data was obtained; see solid line in figure 10. The calculated curve deviates somewhat from the observed data near 940 cm^{-1}. From group theory considerations, the 980 cm^{-1} ν_1 vibrational mode of $SO_4^{=}$ is not expected to be infrared active in liquid droplets. Therefore, we interpret the spectrum shown in figure 10 as due to an 1110 cm^{-1} ν_3 $SO_4^{=}$ absorption (specific absorption of 0.5 m^2/g at the $R_9(28)$ CO_2 laser line) superimposed on a constant background particulate absorption due to water. Assuming the absorption at 920 cm^{-1} to be due totally to particulate water, we estimate that the molar ratio of water to sulfate in our droplets to be approximately 2 : 1. These values are consistent with that expected from wet droplets partially dried in a 50 to 60 % humidity environment and illustrates the capability of this approach. Had we also employed a helium neon 3.39 μm laser for aerosol heating, the fraction of $(NH_4)^+$ ions could also have been determined.

Conclusions

Two promising photothermal aerosol detection schemes have been described which appear to have significant advantages over existing techniques for absorption measurements. Both PFTIR spectroscopy and photothermally modulated Mie scattering can, depending on the geometry and aerosol system chosen for study, yield particle specific absorption data with exceptional sensitivity; i.e. single particle.

Acknowledgements

The authors gratefully acknowledge useful discussions with Professor C. C. Davis of the University of Maryland and with Dr. W. H. Marlow of B.N.L. This work was supported under the auspices of the United States Department of Energy under Contract No. DE-AC02-76CH00016.

References

1. K. T. Whitby , National Bureau of Standards Special Publication. Methods and Standards for Environmental Measurement, pp165-173 (1977)
2. R. W. Terhune and J. E. Anderson, Optics Letters, 1 , 70 (1977)
3. C. W. Bruce and R. G. Pinnick, Appl. Optics, 16, 1762 (1977)
4. C. C. Davis, Appl. Phys. Lett., 36, 513 (1980)
5. S. J. Petuchowski and C. C. Davis, "High Sensitivity Trace Gas Detection by Phase Fluctuation Optical Heterodyne Spectroscopy", presented at the Conference on Laser Engineering and Optical Systems, San Diego, Calif., Feb. 1980.
6. A. J. Campillo, H-B. Lin, C. J. Dodge and C. C. Davis, Optics Letters, 5, 424 (1980)
7. H-B. Lin, J.S. Gaffney and A. J. Campillo, J. of Chromatography, 205, 205 (1981)
8. C. C. Davis and S. J. Petuchowski, Appl. Optics (in press)
9. C. K. N. Patel and R. J. Kerl, Appl. Phys. Lett., 30, 578 (1977)
10. A. Mayer, J. Comera, H. Charpentier and C. Jauss, All. Optics, 17, 391 (1978)
11. M. Born and E. Wolf, "Principles of Optics", 3rd Edition (Pergamon Press, New York, 1965)
12. J. H. Cole, Appl. Optics, 19 , 1023 (1980)
13. A. J. Campillo, C. J. Dodge and H-B. Lin, submitted to Appl. Optics
14. C. H. Chan, Appl. Phys. Lett., 26, 628 (1975)
15. M. Kerker, "The Scattering of Light and Other Electromagnetic Radiation (Academic Press, New York, 1969)
16. B. Y. Liu and K. W. Lee, Am. Ind. Hyg. Assoc. J., 36 , 861 (1975)

17. W. Schnell and G. Fischer, Appl. Optics, 14, 2058 (1975)
18. I. N. Tang, J. Aerosol Sci., 7, 361 (1976)
19. M. Kerker, Amer. Sci., 62, 92 (1974)
20. J. P. Gordon, R. C. C. Leite, R. S. Moore, S. P. S. Porto and J. R. Whinnery, J. Appl. Phys., 36, 3 (1965)
21. A. J. Campillo and H-B. Lin (in preparation)
22. M. E. Baker, Atm. Environ., 10, 241 (1976)
23. P. T. Cunningham, S. A. Johnson and R. T. Yang, Environ. Sci. and Tech., 8, 131 (1974)